1204 J. Chem. Eng. Data **2005,** *50,* 1204−1211

Thermochemistry of the Ternary Solid Complex $Er(C_5H_8NS_2)_3(C_{12}H_8N_2)$

Sanping Chen, Xiangxin Meng, Gang Xie, Shengli Gao,* and Qizhen Shi

Department of Chemistry, Shaanxi Key Laboratory of Physico-Inorganic Chemistry, Northwest University, Xi'an, Shaanxi 710069, China

A solid complex, $Er(C_5H_8NS_2)_3(C_{12}H_8N_2)$, has been obtained from the reaction of hydrous erbium chloride, ammonium pyrrolidinedithiocarbamate (APDC), and 1,10-phenanthroline (o-phen·H_2O) in absolute ethanol. The enthalpy change of the reaction of complex formation from a solution of the reagents, $\Delta_r H_m^\theta$(sol), and the molar heat capacity of the complex, c_m, were determined at 298.15 K by using an RD-496 III heat conduction microcalorimeter. The enthalpy change of complex formation from the reaction of reagents in the solid phase, $\Delta_r H_m^\theta$(s), was calculated on the basis of an appropriate thermochemical cycle and other auxiliary thermodynamic data. The thermodynamics of the reaction of formation of the complex was investigated via the reaction in solution. Fundamental parameters such as the activation enthalpy, the activation entropy, the activation free energy, the apparent reaction rate constant, the apparent activation energy, the preexponential constant, and the reaction order were obtained by combining the thermochemical data of the reaction and kinetic equations with the data of thermokinetic experiments. The constant-volume combustion energy of the complex, $\Delta_c U$, was determined by an RBC-II-type rotating-bomb calorimeter at 298.15 K. Its standard enthalpy of combustion, $\Delta_c H_m^\theta$, and standard enthalpy of formation, $\Delta_f H_m^\theta$, were calculated.

1. Introduction

Over the past few decades, there has been a significant increase in research on complexes containing the bond "lanthanide−sulfur" because they have potential for use in the ceramics industry and in thin materials.[1] Another reason stems from the challenge that the binary complexes exhibit high sensitivity to moisture, so these complexes should be synthesized under strongly anhydrous conditions.[2] In particular, this class of complexes can be used as precursors to generate the lanthanide sulfide nanocrystallites via the convenient thermodecomposition condition.[3−5]

Because chemical and physical processes are accompanied by heat effects, calorimetry represents a unique technique to gather information about thermodynamics and kinetics.[6] Reaction calorimetry has wide application in thermal and kinetic analyses of chemical reactions in the context of thermal process safety and process development. Although there have been reports on these complexes,[7−10] both structurally and spectroscopically, experimental data on the thermodynamic behaviors of these coordination compounds are sparse.

As an extension of our previous studies on the complexes of lanthanides with ligands containing sulfur, the present work describes the synthesis of a novel complex by the reaction of hydrous erbium chloride with ammonium pyrrolidinedithiocarbamate (APDC) and 1,10-phenanthroline (o-phen·H_2O) in absolute ethanol. The complex was characterized by chemical analysis, elemental analysis, IR spectroscopy, and a TG-DTG technique. The enthalpy change of the reaction in solution and the molar heat capacity of the resultant complex at 298.15 K were determined by a microcalormeter. The enthalpy change of complex formation from the reaction of the reagents in the solid phase was derived from a thermochemical cycle. The thermodynamics of the reaction in solution at different temperatures was investigated, and the thermochemical parameters—the apparent reaction rate constant (k), the apparent activation energy (E), the preexponential constant (A), the reaction order (n), the activation enthalpy ($\Delta H_{\neq}^\theta$), the activation entropy ($\Delta S_{\neq}^\theta$), the activation free energy ($\Delta G_{\neq}^\theta$), and the activation enthalpy ($\Delta_r H_{\neq}^\theta$)—were obtained on the basis of reaction thermodynamic and kinetic equations. The constant-volume combustion energy, $\Delta_c U$, of the complex was measured by an RBC-II rotating-bomb calorimeter at 298.15 K. Its standard enthalpy of combustion, $\Delta_c H_m^\theta$, and standard enthalpy of formation, $\Delta_f H_m^\theta$, were calculated.

2. Experimental Section

Chemicals. $ErCl_3 \cdot 3.46H_2O$ was prepared in our experiment. Ammonium pyrrolidinedithiocarbamate (abbreviated APDC, with a mass fraction higher than 0.9950) and 1,10-phenanthroline (abbreviated o-phen·H_2O, with a mass fraction higher than 0.9950) were commercially obtained from Shanghai Reagent Factory. They were maintained in desiccators over P_4O_{10} before the calorimetric measurements. Absolute ethanol and dichloromethane are of A. R. grade from Xi'an chemical reagent company. Potassium chloride (mass fraction 0.9999) was purchased from Shanghai No. 1 Reagent Factory, Shanghai, China, and dried in a vacuum oven at 500 K for 8 h prior to use. Thianthrene, purchased from Tokyo Kasei Kogyo Co., Ltd, is of GC grade with a purity of 99 %. It was recrystallized with a mass fraction of better than 99.99 % as characterized by HPLC and was stored in desiccator containing P_4O_{10}. The gamma aluminum oxide is of spectroscopic pure grade from Shanghai No.1 Reagent Factory. It was transformed to alpha aluminum oxide in a muffle oven at 1473.15 K prior to use and maintained in desiccator with P_4O_{10}.

---

* Corresponding author. E-mail: gaoshli@nwu.edu.cn.

10.1021/je0495738 CCC: $30.25

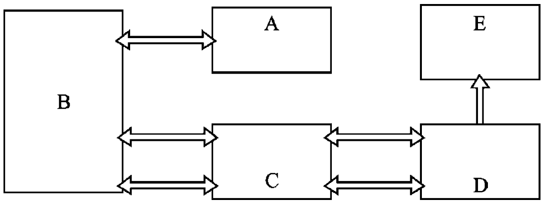

Figure 1. Schematic view of an RD496-III microcalorimeter: (A) main body; (B) temperature control, microvolt amplifier, and calibration system; (C) modulus; (D) computer; (E) printer.

The relative atomic masses used were those recommended by the IUPAC Commission in 1999.[11]

Equipment and Analytical Methods. The Er^{3+} content was determined volumetrically with EDTA by complexometric titration, the Cl^{-1} content was determined by $AgNO_3$ titration; C, H, N, and S contents were determined by a Vario EL III CHNOS instrument (Germany). Spectra were obtained with samples in a KBr matrix for the title complex and ligands. A BEQ UZNDX-550 series FT-IR spectrophotometer in the region from 400 cm^{-1} to 4000 cm^{-1} was used. The TG-DTG tests were performed from 303.15 K to 773.15 K in a Perkin-Elmer thermobalance and under a dynamic atmosphere of high-purity N_2 (mass fraction 0.99999) with a flow rate of 60 cm^3 min^{-1} and a heating rate of 10 K min^{-1}. The ICP-OES spectroscopy was carried out to check the progress of the reaction occurring in the calorimetric experiments using a Perkin-Elmer ICP Liberty 150 instrument. The phase structure of the solid combustion product was identified by a Rigua D/max-III C X-ray diffractometer using Cu Kα radiation. A D/max-III-type X-ray power diffractometer type with Cu Kα radiation was used. The calorimetric experiments were performed using a RD496-III-type microcalorimeter and an RBC-II-type rotating-bomb calorimeter.[12,13] The purity of the compound was verified by an HP-1100-type high-performance liquid chromatography analyzer; the solvent was CH_2Cl_2, the rinsing reagent was CH_2Cl_2, and the column was contra-phase carbon-18.

RD496-III Heat Conduction Calorimeter. All of the enthalpies of solutions and those of reactions were measured with an RD496-III microcalorimeter.[12] The heat conduction microcalorimeter is mainly composed of the precision temperature-controlling system, the electric energy calibration system, the constant-temperature thermostat, and the data processing system, which is shown schematically in Figure 1. The working temperature of the calorimeter lies in the range of $T = (77.15 \text{ to } 473.15)$ K. It has a 16 mL sample cell and a 16 mL reference cell. The thermal effect can be determined through a thermoelectric pile composed of 496 thermocouples, which is converted to thermal electric potential. The thermal electric potential is amplified through a microvolt amplifier, converted by the modulus, collected, and processed by a computer. The functions of controlling the temperature of the system, running on chemical and electrical calibrations, having the sensitivity calibrated, measuring the thermal effect, and picking up and saving the results are achieved by a program under a Windows system developed by us.

The baseline stability was determined at a constant temperature and with rising temperature at a stated heating rate. Keeping the temperature at 313.15 K for 50 h, we found that the baseline change was less than ±0.2 μV. Raising the temperature from 73.15 K to 313.15 K at the speed of 1 K h^{-1}, we observed that the stability is 0.4 μV K^{-1}.

Table 1. Enthalpy of Solution of KCl in Deionized Water at 298.15 K

no. of experiments	m/g	r	$\Delta_{sol}H_m^\theta$/kJ mol^{-1}
1	0.0663	499	17.602
2	0.0667	496	17.646
3	0.0670	494	17.677
4	0.0660	502	17.475
5	0.0664	499	17.474
6	0.0661	501	17.612
$(\bar{x} \pm \sigma_a)^a$			17.581 ± 0.039
literature[13]			17.584 ± 0.007

[a] $\sigma_a = \sqrt{\sum_{i=1}^{6}(x_1-\bar{x})^2/n(n-1)}$, in which n is the experimental number, x_i is a simple value in a set of dissolution measurements, $\bar{x}$ is the mean value of a set of measurement results, and r is the molar ratio of $n(H_2O)$ to $n(KCl)$.

The calorimetric constants at (292.15, 295.15, 298.15, and 301.15) K were determined by the Joule effect before the experiments and are (63.691 ± 0.035), (63.799 ± 0.042), (63.901 ± 0.030), and (64.000 ± 0.026) μV mW^{-1}, respectively. The reliability of the calorimeter was verified by measuring the dissolution enthalpy of KCl (calorimetric primary standard) in double-distilled water at 298.15 K. According to the molar ratio of KCl to H_2O, $n_{KCl}/n_{H_2O} \approx 1{:}500$, a known amount of KCl is dissolved in double-distilled water at (298.15 ± 0.001) K. The average enthalpy of dissolution of KCl, $\Delta_s H^\theta_{m,KCl}$, determined from the six tests, is (17.581 ± 0.039) kJ mol^{-1}, as shown in Table 1, which is in agreement with the published value of (17.584 ± 0.007) kJ mol^{-1}.[13]

RBC-II Rotating-Bomb Combustion Calorimeter. The constant-volume combustion energy of the compound was measured by an RBC-II-type precise rotating-bomb combustion calorimeter.[14] A schematic diagram of the microcombustion bomb developed in our laboratory is shown in Figure 2. It mainly consists of a thermostatic trough with an outer casing, a calorimetric tube, and a system for temperature measurement. The volume of the thermostatic trough was about 25.0 dm^3, and it was equipped with two interior agitators. The temperature of the thermostatic water in the bath is automatically maintained at (298.15 ± 0.001) K by means of a precise thermoresistor. The volume of the calorimetric tube is 4.5 dm^3. The temperature gauge from the digital indicator with an integrated circuit is used to measure the temperature of the calorimetric tube. The bicyclic structure of the

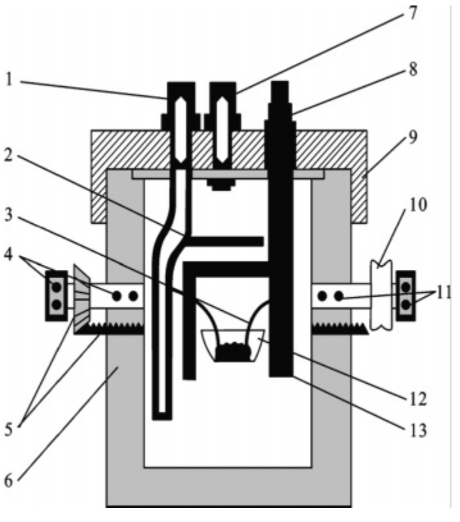

Figure 2. Transversal view of the rotating bomb: (1) gas-filled valve; (2) flame baffle; (3) Ni−Cr wire for ignition; (4) ball; (5) bevel gear; (6) bomb body; (7) exhaust valve; (8) electrode; (9) bomb cover; (10) pulley; (11) ball bearing; (12) crucible; (13) crucible support.

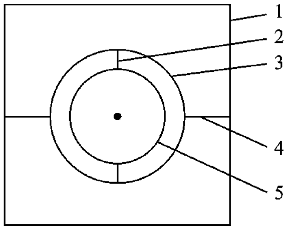

Figure 3. Bicyclic structure of the crucible support in the oxygen bomb: (1) support; (2) *x* axle; (3) outside ring; (4) *y* axle; (5) inside ring.

crucible support in the oxygen bomb, as shown in Figure 3, is constructed so that the bomb can make a compound rotation about an axis perpendicular to the bomb axis (i.e., end-over-end rotation) and about the bomb axis (axial rotation) at the same time.

When the temperature of the thermostatic water bath of the outer casing was regulated at (298.15 ± 0.001) K, the temperature of the water in the calorimetric tube was adjusted to a temperature lower than that of the water bath of the outer casing. It is assured that the range of the temperature change in the calorimetric tube is half of the total temperature rise of the calorimeter after the combustion is complete. The bomb was sealed after adding a known amount of pure water to the calorimetric tube, putting the sample into the crucible fixed onto the support in the rotating bomb but not in contact with the solution, fastening the combustion fuse in the support pillars of the bomb, injecting the initial bomb solution into the rotating bomb, and filling the bomb with 2.533 MPa of oxygen per period. It is important for the temperature change of the calorimeter to remain constant at the beginning of each experiment. During the initial stage of the experiment, the temperature reading was recorded thirty times every 30 s. After that, the sample was ignited, and the temperature reading was recorded one time per minute until the rate of the temperature change stayed constant. The main period of the combustion reaction was finished at this stage. During the final stage of the experiment, the temperature reading was recorded 30 times every 30 s.

The temperature rise must be corrected on the basis of the heat exchange between the calorimetric tube and its surroundings. The correction value of the heat exchange was calculated by means of the following equation in the literature:[15]

$$\varsigma = \left(\frac{V_n - V_0}{\theta_n - \theta_0}\right)\left(\frac{T_0 + T_n}{2} + \sum_{i=1}^{n-1} T_i - n\theta_n\right) + nV_n \qquad (1)$$

where ς (K) denotes the correction value of the heat exchange; n, the number of readings for the main (or reaction) stage; V_n (K min^{-1}) and V_0 (K min^{-1}), the temperature drift rates in the final and initial stages, respectively (V is positive when the temperature decreases); θ_n (K) and θ_0 (K), the average temperatures of the calorimeter during the final and initial stages, respectively; T_0 (K), the last reading of the initial stage; T_n (K), the first reading of the final stage; $\sum_{i=1}^{n-1} T_i$, the sum of all of the temperature readings, except for the last one, of the main stage; and $(V_n - V_0)/(\theta_n - \theta_0)$, a constant related to the calorimeter performance.

After the experiment was over, the final products of the combustion reaction were analyzed.[14]

The gaseous sulfurous anhydride produced during the process of the combustion reaction was converted catalytically to sulfur trioxide, where the platinum lining of the interior surfaces of the bomb was acting as a catalyst. The bomb solution then absorbed the gaseous sulfur trioxide, generating aqueous sulfuric acid. The amount of sulfuric acid was determined by the gravimetric $BaSO_4$ method.

The remains of the gases formed in the combustion were collected in a gas-collecting bag. The volume was measured by a gas meter that was fitted between the bag and the bomb. The gaseous carbon dioxide produced in the combustion was absorbed by a weighted absorption tube containing alkali asbestos. The amount of CO_2 was determined through the weight increment of the tube after absorbing the carbon dioxide. The amount of CO_2 dissolved in the final solution was neglected. Four absorption tubes were connected in series with each other for the vapor measurement. The first was filled with P_4O_{10} and $CaCl_2$ (anhydrous) to absorb the water vapor contained in the gas, the second was filled with active MnO_2 to absorb the nitrogen oxides, the third was filled with alkali asbestos to absorb the CO_2, and the fourth was full of the solid P_4O_{10} and $CaCl_2$ (anhydrous) to absorb the water vapor formed in the determination. The nitrogen oxides (NO_x) produced from the oxidation of a trace amount of nitrogen contained in the bomb mainly existed in the form of NO_2 because of the excess oxygen in the bomb, as shown by the results obtained according to the procedure in the literature.[14] No NO_2 appeared in the gas phase because it was readily dissolved in the water poured into the bottom of the bomb to form the aqueous nitric acid.

The fittings and the interior surfaces of the bomb were washed three times using distilled water at first, after which the bomb solution including the washing solution was completely transferred to a conical bottle and heated to boiling to remove a small amount of CO_2 dissolved in the bomb solution. The total amount of nitric acid was obtained from titrating the solution to a phenothalin end point with a standard solution of NaOH. Because the crucible in the rotating bomb was attached to the support, the final solid products were left in the crucible at the end of the experiment. The results of the IR spectra, XRD, and chemical and elementary analyses have shown that the final solid product was only cubic erbium sesquioxide. The analyses of the combustion products indicated that the compound was combusted to CO_2(g), H_2O(l), H_2SO_4(aq), and Er_2O_3(s) under excess oxygen. The amounts of NO_x and CO in the final gas phase may be neglected.

The energy equivalent of the RBC- II-type calorimeter, ϵ_{calor}, was determined from six combustion experiments using about 0.8 g of NIST 39i benzoic acid with a certified mass energy of combustion of $\Delta_c U = -(26\,434 \pm 3)$ J g^{-1} under the same experimental conditions to be (17 775.1 ± 7.4) J K^{-1} by eq 2. The calibrated experimental results with an uncertainty of 4.68×10^{-4} are summarized in Table 2:

$$\epsilon_{\text{calor}} = \frac{\Delta_c U a + G b + 59.8 V N}{\Delta T} \qquad (2)$$

where ϵ_{calor} (J K^{-1}) is the energy equivalent of the calorimeter; $\Delta_c U$ (J g^{-1}), the mass energy of combustion of benzoic acid; a (g), the mass of a pellet of benzoic acid; G (J cm^{-1}), the combustion enthalpy of Ni−Cr wire for ignition (G = 0.9 J cm^{-1}); b (cm, the length of the actual Ni−Cr wire consumed in ignition; 59.8 (kJ mol^{-1}), the energy of formation of aqueous nitric acid based on the molar energy of formation of HNO_3(aq) from N_2(g), O_2(g), and H_2O(l), where $\Delta_d H_m^0$ is of 59.8 kJ mol^{-1} for 0.1 mol dm^{-3} HNO_3(aq);[14,15] V (cm^3), the volume of the consumed sodium hydroxide solution; N (mol dm^{-3}), the molar concentration of the sodium hydroxide solution used in the neutral titration

Table 2. Results for the Calibration of the Energy Equivalent of the Rotating-Bomb Calorimeter at 298.15 K

no.	mass of complex m/g	calibrated heat of combustion of the wire q_c/J	calibrated heat of acid q_N/J	calibrated ΔT/K	energy equiv W/J K^{-1}
1	0.99702	10.35	24.78	1.4834	17 790.45
2	0.78940	8.10	20.89	1.1746	17 789.88
3	0.83060	12.60	20.43	1.2382	17 758.93
4	0.96869	12.60	17.43	1.4418	17 780.82
5	0.99485	12.60	20.80	1.4800	17 798.18
6	1.12328	9.09	21.85	1.6735	17 761.41
7	0.90036	9.28	21.67	1.3429	17 745.97
($\bar{x} \pm \sigma_a$)					17 775.09 ± 7.43

Table 3. Experimental Results for the Combustion Energies of the Complex $Er(C_5H_8NS_2)_3(C_{12}H_8N_2)$ and Thianthrene

compound	no. of experiments	mass of complex m/g	calibrated heat of combustion of the wire Q_c/J	calibrated heat of acid Q_N/J	calibrated ΔT/K	combustion energy of the complex $-\Delta_cU$/J g^{-1}
$Er(C_5H_8NS_2)_3(C_{12}H_8N_2)$	1	0.81204	11.70	2036.12	1.0136	19 665.30
	2	0.83050	11.70	2073.30	1.0345	19 630.74
	3	0.80342	10.80	2018.76	1.0001	19 600.34
	4	0.80586	12.60	2023.66	1.0031	19 598.85
	5	0.81350	12.60	2039.03	1.0142	19 638.43
	6	0.82687	12.60	2065.93	1.0309	19 647.36
	($\bar{x} \pm \sigma_a$)					19 630.55 ± 10.53
thianthrene	1	0.48860	12.60	1383.69	0.9998	33 514.62
	2	0.48886	11.70	1384.41	1.0015	33 558.98
	3	0.49011	12.60	1387.90	1.0028	33 511.58
	4	0.48798	12.60	1381.96	0.9977	33 484.26
	5	0.48835	12.60	1382.99	0.9977	33 456.78
	6	0.48823	12.60	1382.65	0.9992	33 520.31
	($\bar{x} \pm \sigma_a$)					33 507.76 ± 14.13

Table 4. Main XRD Data of the Title Complex $Er(C_5H_8NS_2)_3(C_{12}H_8N_2)$ with Ligands *o*-phen·H_2O and APDC

compound	main X-ray powder diffraction data								
APDC	I/I_0	40	100	12	26	62	10	20	13
	d/nm	0.1099	0.5507	0.4736	0.4107	0.3675	0.2877	0.2641	0.2206
o-phen·H_2O	I/I_0	46	26	54	99	72	34	25	33
	d/nm	0.8909	0.6189	0.5169	0.4454	0.3959	0.3847	0.3149	0.2817
$Er(C_5H_8NS_2)_3(C_{12}H_8N_2)$	I/I_0	71	54	100	58	44	98	64	82
	d/nm	9.839	8.615	7.894	6.692	5.719	4.881	4.207	3.890

of the nitric acid, where N is often 0.1000 mol dm^{-3}; and ΔT, the corrected temperature rise of the combustion or reaction, where ΔT equals $(T_n - T_0) + \varsigma$, as obtained from eq 1.

To evaluate the precision and accuracy of the measurement of the standard energy of combustion for the compound involving sulfur, the standard energy of combustion of thianthrene was determined, using our rotating-bomb set, to be −(33 507.8 ± 14.1) J g^{-1} as shown in Table 3.

Synthesis of the Complex. $ErCl_3 \cdot 3.46H_2O$, *o*-phen·H_2O, and APDC (molar relation 1/1/3 salt/phen/APDC) were dissolved independently in a minimal amount of absolute ethanol. To the mixed ethanolic solution of *o*-phen·H_2O and APDC, the ethanolic solution of the salt was slowly added dropwise under electromagnetic stirring. The reaction mixture was allowed to stand for 30 min, resulting in the formation of a solid that was filtered, washed with three small portions of absolute ethanol, and purified with CH_2Cl_2. The resulting crystals were dried in vacuum and stored in a desiccator over P_4O_{10} ready to be used.

3. Results and Discussion

Characterization of the Complex. The elemental analyses results of the title complex are as follows: w(calcd): Er 21.27 %, C 41.25 %, H 4.10 %, N 8.91 %, S 24.47 %; w (found): Er 21.01 %, C 41.12 %, H 4.06 %, N 8.79 %, S 24.43 %, which is identified as the formula for $Er(C_5H_8NS_2)_3(C_{12}H_8N_2)$. The complex was checked by HPLC, and its purity is excellent (mass fraction 0.9999).

The main XRD data of ligands and the complex are shown in Table 4. Clearly, the main XRD data of the complex are very different from that of hydrous erbium chloride (L. C. D. D. card) and ligands, indicating that the complex is a new phase.

The preliminary identification regarding the nature of bonding of ligands *o*-phen·H_2O and APDC to the erbium ion has been obtained from the IR data. Figure 4 shows the IR spectra of the salt, ligands, and complex. The IR spectra reveal that both ligands—*o*-phen·H_2O and APDC—are coordinated to the metal ion.[16,17] Comparing with the spectra of salt (a) and *o*-phen·H_2O (b), the characteristic absorption band attributed to the stretching vibration of

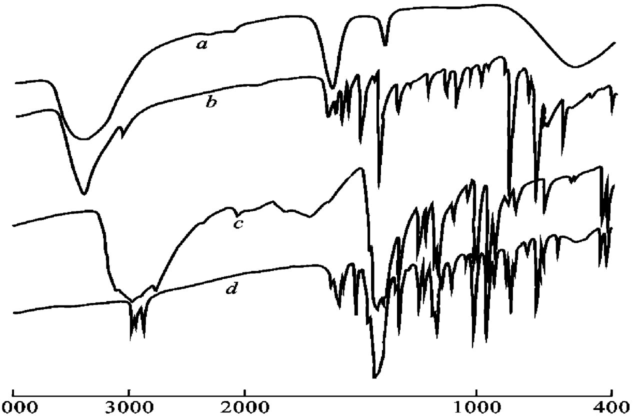

Figure 4. Comparison of IR spectra of (a) $ErCl_3 \cdot 3.46H_2O$, (b) *o*-phen·H_2O, (c) APDC, and (d) complex $Er(C_5H_8NS_2)_3(C_{12}H_8N_2)$.

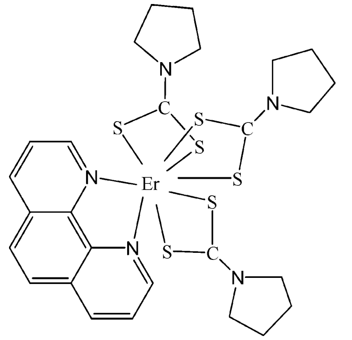

Figure 5. Presumed structure of complex $Er(C_5H_8NS_2)_3(C_{12}H_8N_2)$.

the hydroxyl group of water molecules is observed at 3390 and 3388 cm^{-1}, respectively. This band is not observed in the complex spectrum. The IR spectrum of the complex showed absorption bands at 1625, 1590, 1574, and 1517 cm^{-1}, which are attributed to the skeleton vibration of the benzene ring when compared with that of free phen. Absorption bands at 844 and 727 cm^{-1} are attributed to the bending vibration of the C−H group in the complex. These vibrations are found to be shifted to higher frequencies in the complex relative to those in free phen, suggesting the coordination of two nitrogen atoms of *o*-phen to Er^{3+}. In contrast with the absorption band found at 1417 cm^{-1} in the ligand APDC (c), the stretching vibration of the group CN (ν_{CN}) shifts to the higher frequency of 1434 cm^{-1}, characterizing the double-bond character of the CN bond. The $C_4H_8NCSS^-$ ion may be represented by a resonance hybrid of the structures[8,18]

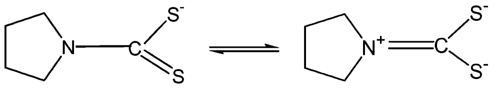

The second structure is favored when the two sulfur atoms of the ligand coordinate to Er^{3+} to form a four-membered ring;

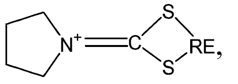

accordingly, ν_{CN} moves to a higher frequency. Additionally, corresponding to the peak of 938 cm^{-1} ascribable to the charcteristic absorption of $-$ CSS^{2-} in the ligand of APDC, it splits into two peaks of 1011 and 949 cm^{-1} in the complex. Obviously, the resulting four-membered ring increases the vibration intensity of υ_{CN}.[17] The changes in ν_{CN} and ν_{CSS} indicate that the two sulfur atoms of the ligand coordinate to Er^{3+}, with $C_4H_8NCSS^-$ being a bidentate ligand. We assume that the structure of the complex is that shown in Figure 5.

Thermostability of the Solid Complex. The TG-DTG curve of the complex is presented in Figure 6. The complex is decomposed into the final compounds in one step, which begins at 303.15 K and is complete 738.15 K, accompanying by a mass loss of 69.57 %. To explore the decomposition process of the title complex, the final compounds determined by XPS are of the mixture of Er_2S_3 and deposited carbon in which Er_2S_3 predominates.[19] On the basis of the above analyses, the decomposition process is postulated as eq 3, where 501.15 K is the peak value in the DTG curve and 30.45% is the calculated value of the mass residual. Clearly, the experimental result is in good agreement with the calculated result.

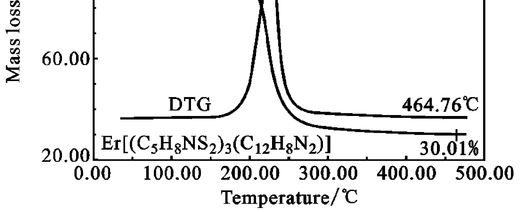

Figure 6. TG-DTG curve of complex $Er(C_5H_8NS_2)_3(C_{12}H_8N_2)$.

$$Er[(C_5H_8NS_2)_3(C_{12}H_8N_2)] \xrightarrow[30.43\ \%\ (30.45\ \%)]{303.15\ K-501.15\ K-738.15\ K} \frac{1}{2}\,Er_2S_3 + 2C \quad (3)$$

Calculation of the Standard Molar Enthalpy Change for the Reaction in the Solid State. The molar enthalpies of solution $\Delta_{sol}H^{\theta}_{m}(1)$, $\Delta_{sol}H^{\theta}_{m}(2)$, and $\Delta_{sol}H^{\theta}_{m}(3)$ of $ErCl_3{\cdot}3.46H_2O$, APDC, and *o*-phen·H_2O in absolute ethanol at 298.15 K, respectively, are given in Table 5. The mixed enthalpy of the mixture of the two ethanolic solutions of the ligands $\Delta_{mix}H^{\theta}_{m}$ and the enthalpy change for the reaction in solution $\Delta_rH^{\theta}_{m}(sol)$ are listed in Table 6. The enthalpy of dissolution, $\Delta_{sol}H^{\theta}_{m}(4)$ of water in ethanol is so small that it can be regarded as zero.

The the application of Hess' law to the series of equations shown in Table 7 gives a thermochemical cycle from which the enthalpy change of the reaction in the solid state is derived as being (16.1 ± 0.4) kJ mol^{-1} according to eq 4, where the uncertainty is given as the standard deviation of the mean.

$$\begin{aligned}\Delta_rH^{\theta}_{m}(s) &= \Delta_{sol}H^{\theta}_{m}(1) + 3\Delta_{sol}H^{\theta}_{m}(2) + \Delta_{sol}H^{\theta}_{m}(3) + \\ &\quad \Delta_{mix}H^{\theta}_{m} + \Delta_rH^{\theta}_{m}(l) - \Delta_{sol}H^{\theta}_{m}(4) \\ &= [(-45.714 \pm 0.196) + 3(19.538 \pm 0.090) + \\ &\quad (20.970 \pm 0.071) + (10.592 \pm 0.049) + \\ &\quad (-28.318 \pm 0.060) - 0]\ kJ\ mol^{-1} \\ &= (16.1 \pm 0.4)\ kJ\ mol^{-1} \qquad (4)\end{aligned}$$

Some efforts have been devoted to test the reasonability of the thermochemistry cycle. The crude products of the liquid-phase reactions from the calorimetric experiments were collected and separated by the centrifugal effect. The solid crude products were purified and identified as being the same product as that obtained in the direct synthesis The concentration of Er^{3+} retained in the centrifugal liquid was determined to be 6 × 10^{-3} μg mL^{-1} by the ICP-AES experiment, indicating that the starting reactants have been transformed fully to the title products; that is, the liquid-phase reaction proceeds to 100 %. All of these indicate that the final thermodynamic states of the title solid-phase reaction and that of the liquid-phase reaction are the same and that the designed thermochemistry cycle is correct.

Calculation of the Thermodynamic Parameters for the Reaction in the Liquid State. The calorimetric experiment showed that this reaction is an exothermic one. On the basis of thermokinetic data of the reaction in solution at different temperatures as shown in Table 8 and the thermodynamic equations,[6] the thermodynamic parameters and kinetic parameters of the reaction in solution are obtained and shown in Table 9.

Molar Heat Capacity of the Complex. To obtain the value of the molar heat capacity of the solid compound, the empty cell (system I), the cell containing a sample with an

Table 5. Enthalpies of Solution of $ErCl_3·3.46H_2O$, Ammonium Pyrrolidinedithiocarbamate (APDC), and 1,10-Phenanthroline (*o*-phen·H_2O) in Absolute Ethanol at 298.15 K

	m	Q	$\Delta_{sol}H^{\theta}_{m}(1)$[a]	m	Q	$\Delta_{sol}H^{\theta}_{m}(2)$[b]	m	Q	$\Delta_{sol}H^{\theta}_{m}(3)$[c]
no.	mg	mJ	kJ mol^{-1}	mg	mJ	kJ mol^{-1}	mg	mJ	kJ mol^{-1}
1	80.66	−10 944.216	−45.583	26.29	3099.238	19.368	31.71	3351.540	20.950
2	80.59	−10 870.105	−45.313	26.25	3121.801	19.539	31.77	3393.602	21.173
3	80.68	−11 098.503	−46.214	26.27	3171.104	19.832	31.76	3343.271	20.866
4	80.63	−11 074.625	−46.143	26.24	3082.010	19.297	31.73	3356.008	20.965
5	80.58	−11 005.231	−45.882	26.33	3157.941	19.705	31.68	3315.208	20.746
6	80.59	−10 830.292	−45.147	26.28	3117.297	19.488	31.73	3379.615	21.123
($\bar{x} \pm \sigma_a$)			−45.714 ± 0.196			19.538 ± 0.090			20.970 ± 0.071

[a] $\Delta_{sol}H^{\theta}_{m}(1)$ represents the enthalpy of solution of $ErCl_3·3.46H_2O$ in absolute ethanol. [b] $\Delta_{sol}H^{\theta}_{m}(2)$ represents the enthalpy of solution of APDC in absolute ethanol. [c] $\Delta_{sol}H^{\theta}_{m}(3)$ represents the enthalpy of solution of *o*-phen·H_2O in absolute ethanol.

Table 6. Mixed Enthalpy of the Ethanolic Solution of APDC and *o*-phen·H_2O and the Enthalpy Change of the Reaction in the Liquid State, $\Delta_rH^{\theta}_{m}$(sol) ($ErCl_3·3.46\ H_2O$)·xC_2H_5OH(l) + [3APDC·yC_2H_5OH(l) + [(*o*-phen·H_2O)·zC_2H_5OH(l)] = Er(PDC)$_3$ (*o*-phen)(s) + 3NH_4Cl(s) + 4.46H_2O·(x + 3y + z)C_2H_5OH(l), at 298.15 K

	Q_1	$\Delta_{mix}H^{\theta}_{m}$	Q_2	$\Delta_rH^{\theta}_{m}(1)$[b]
no.	mJ	kJ mol^{-1a}	mJ	kJ mol^{-1}
1	84.809	10.601	−226.360	−28.295
2	86.293	10.787	−227.485	−28.436
3	84.231	10.529	−225.215	−28.152
4	86.064	10.508	−227.856	−28.482
5	83.987	10.498	−226.876	−28.360
6	85.006	10.626	−225.438	−28.180
($\bar{x} \pm \sigma_a$)	85.065 ± 0.421	10.592 ± 0.049	−226.538 ± 0.479	−28.318 ± 0.060

[a] $\Delta_{mix}H^{\theta}_{m}$ is the mixed enthalpy of the ethanolic solution of APDC and *o*-phen·H_2O. [b] $\Delta_rH^{\theta}_{m}$(l) is the enthalpy change of the liquid-phase reaction ($ErCl_3·3.46H_2O$)·xC_2H_5OH(l) + 3APDC·yC_2H_5OH(l) + [(*o*-phen·H_2O)·zC_2H_5OH(l) = Er(PDC)$_3$ (*o*-phen)(s) + 3NH_4Cl(s) + 4.46H_2O·(x + 3y + z)C_2H_5OH(l).

Table 7. Thermochemical Cycle and Results for ΔH^{θ}_{m}

reaction	ΔH^{θ}_{m}/kJ mol^{-1}
1 $ErCl_3·3.46\ H_2O$(s) + xC_2H_5OH(l) = ($ErCl_3·3.46H_2O$)·xC_2H_5OH(l)	−45.714 ± 0.196
2 3APDC(s) + yC_2H_5OH(l) = 3(APDC·yC_2H_5OH)(l)	19.538 ± 0.090
3 *o*-phen·H_2O(s) + zC_2H_5OH(l) = (*o*-phen·H_2O)·zC_2H_5OH(l)	20.970 ± 0.071
4 [3APDC·yC_2H_5OH(l)] + [(*o*-phen·H_2O)·zC_2H_5OH(l)] = (3APDC)(*o*-phen·H_2O)·(y + z)(C_2H_5OH)(l)	10.592 ± 0.049
5 [($ErCl_3·3.46H_2O$)·xC_2H_5OH(l) + 3APDC·yC_2H_5OH(l) + [(*o*-phen·H_2O)·zC_2H_5OH(l)] = Er(PDC)$_3$(*o*-phen)(s) + 3NH_4Cl(s) + 4.46H_2O·(x + 3y + z)C_2H_5OH(l)	−28.318 ± 0.060
6 4.46H_2O + (x + 3y + z)C_2H_5OH(l) = 4.46H_2O·(x + 3y + z)C_2H_5OH(l)	0
7 $ErCl_3·3.46H_2O$(s) + 3APDC(s) + *o*-phen·H_2O(s) = Er(PDC)$_3$(*o*-phen)(s) + 3 NH_4Cl(s) + 4.46H_2O	16.144 ± 0.350

Table 8. Thermokinetic Data of the Liquid-Phase of Formation Reaction ($ErCl_3·3.46H_2O$)·xC_2H_5OH(l) + [3APDC·yC_2H_5OH(l) + [(*o*-phen·H_2O)·zC_2H_5OH(l)] = Er(PDC)$_3$(*o*-phen)(s) + 3NH_4Cl(s) + 4.46H_2O·(x + 3y + z)C_2H_5OH(l)

292.15 K			295.15 K			298.15 K			301.15 K		
		dH_i/dt			dH_i/dt			dH_i/dt			dH_i/dt
t/s	H_i/H_0[a]	10^{-4} J s^{-1}	t/s	H_i/H_0[a]	10^{-4} J s^{-1}	t/s	H_i/H_0[a]	10^{-4} J s^{-1}	t/s	H_i/H_0[a]	10^{-4} J s^{-1}
185	0.2680	8.2787	165	0.3526	7.4923	220	0.5997	5.6181	50	0.1320	8.0938
190	0.2766	8.2198	170	0.3649	7.4139	225	0.6120	5.5242	55	0.1513	7.9844
195	0.2853	8.1610	175	0.3771	7.3199	230	0.6241	5.4146	60	0.1704	7.8750
200	0.2939	8.1022	180	0.3891	7.2415	235	0.6360	5.3051	65	0.1894	7.7656
205	0.3024	8.0434	185	0.4010	7.1631	240	0.6476	5.1955	70	0.2080	7.6719
210	0.3109	7.9848	190	0.4128	7.0691	245	0.6590	5.1016	75	0.2264	7.5625
215	0.3193	7.9132	195	0.4244	6.9907	250	0.6702	4.9921	80	0.2444	7.4531
220	0.3277	7.8680	200	0.4359	6.8967	255	0.6811	4.8826	85	0.2621	7.3438
225	0.3359	7.8101	205	0.4472	6.8183	260	0.6918	4.7887	90	0.2794	7.2500
230	0.3441	7.7523	210	0.4584	6.7399	265	0.7023	4.7104	95	0.2963	7.1406

[a] H_0 = 0.3471J (292.15 K), 0.2735 J (295.15 K), 0.2264J (298.15 K), and 0.1649J (301.15 K).

unknown specific heat c (system II), the cell containing the first standard substance with a known specific heat c_1 (system III), and the cell containing the second standard substance with known specific heat c_2 (system I) are uniformly heated by the same Peltier current for 1 h. When thermal equilibrium of systems I−IV is established, it can be shown that (a) the temperature is uniform within the cell and (b) the equilibrium temperature θ is the same for a given Peltier current, whatever the cell contents. When the Peltier current is turned off, the quantities of heat q_0, q, q_1, and q_2 retained by systems I−IV are given by eqs 5−8:

for system I $$q_0 = a\theta \tag{5}$$

for system II $$q = (a + mc)\theta \tag{6}$$

for system III $$q_1 = (a + m_1c_1)\theta \tag{7}$$

for system IV $$q_2 = (a + m_2c_2)\ \theta \tag{8}$$

Table 9. Kinetic and Thermodynamic Parameters of Liquid-Phase Reaction ($ErCl_3 \cdot 3.46H_2O$)·xC_2H_5OH(l) + [3APDC·yC_2H_5OH(l) + [(*o*-phen·H_2O)·zC_2H_5OH(l)] = Er(PDC)$_3$(*o*-phen)(s) + 3NH_4Cl(s) + 4.46H_2O·(x + 3y + z)C_2H_5OH(l)

T/K	$k \times 10^3$/s^{-1}	n	r	E/kJ mol^{-1}	ln A	r[a]	$\Delta G_{\neq}^{\theta}$/kJ mol^{-1}	$\Delta H_{\neq}^{\theta}$/kJ mol^{-1}	$\Delta S_{\neq}^{\theta}$/J mol^{-1} K^{-1}	r[a]
292.15	2.8764	0.6004	0.9995	50.08	14.767	0.9999	85.71	47.614	−130.408	0.9998
295.15	3.5532	0.5976	0.9997				86.10			
298.15	4.3347	0.6085	0.9992				86.51			
301.15	5.3386	0.5942	0.9998				86.88			

[a] r − linear correlation coefficient.

Table 10. Experimental Data Used for Calculating the Molar Heat Capacity of the Complex c_m at 298.15 K

experimental data	empty cell	benzoic acid	α-Al_2O_3	Er(PDC)$_3$(*o*-phen)
q/mJ	4453.908	6088.611	4959.916	5015.753
	4444.543	6080.422	4962.776	5014.046
	4432.133	6094.207	4977.771	4991.327
	4447.035	6098.640	4984.568	4994.721
	4438.165	6075.115	4967.144	4984.811
	4450.647	6073.035	4983.760	4980.451
($\bar{x} \pm \sigma_a$)	4444.405 ± 3.610	6085.005 ± 4.672	4972.656 ± 4.824	4996.852 ± 6.639
precision ($\sigma_a/\bar{x}$)	1.816×10^{-3}	1.717×10^{-3}	2.169×10^{-3}	2.971×10^{-3}
m/g		4.51478	2.68416	2.44852
c/J mol^{-1} K^{-1}		78.707 ± 2.927	145.923 ± 0.562	90.419 ± 1.544
c_0 from lit./J mol^{-1} K^{-1}		79.03[20]	145.327[21]	
accuracy $(c_0 - c)/c_0$		4×10^{-3}	4×10^{-3}	

where a (J K^{-1}) is the apparent heat capacity of the empty cell; θ (K) is the equilibrium temperature for a given Peltier current; m (g), m_1(g), and m_2(g) are the masses of the investigated sample, the first standard substance, and the second standard substance, respectively; c (J mol^{-1} K^{-1}), c_1(J mol^{-1} K^{-1}), and c_2 (J mol^{-1} K^{-1}) are the molar heat capacity of the investigated sample, the first standard substance, and the second standard substance, respectively; and q_0 (J), q (J), q_1 (J), and q_2 (J) are the quantities of heat retained by systems I−IV when they were heated by a given Peltier current.

From a combination of eqs 5−8, eq 9 is obtained:

$$c = \left(\frac{q - q_0}{2m}\right)\left(\frac{m_1 c_1}{q_1 - q_0} + \frac{m_2 c_2}{q_2 - q_0}\right) \quad (9)$$

The value of c of the investigated sample can be obtained from eq 9 if the values of c_1 and c_2 of two standard substances are known.

The molar heat capacity of the complex is determined by an RD496-III-type microcalorimeter when changing the samples in the sample cell. The values of q are obtained by the testing method presented as a thermogram in Figure 7. In Figure 7, AG is the baseline; at time B, a constant Peltier current is generated in the laboratory cell; at CD, the steady state of the system is established; at point D, the Peltier effect is turned off; at point E, the state of the system has returned to the experimental initial state after turning off the Peltier current; and q is the total heat, as shown as the shadow area. Therefore, the molar heat capacity of the sample is derived from eq 9. The results of the experiments are shown in Table 10.

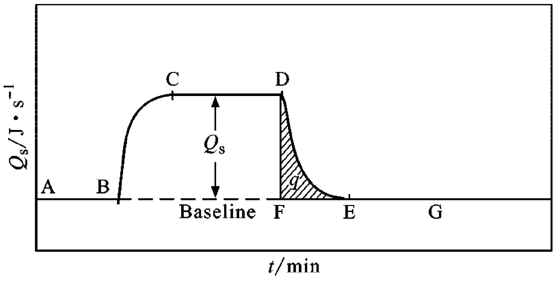

Figure 7. Thermogram of measurement of the molar heat capacity of complex Er($C_5H_8NS_2$)$_3$($C_{12}H_8N_2$).

Combustion Energy of the Complex. The determination method of the combustion energy of the complex was the same as for the calibration of the calorimeter with benzoic acid. The combustion energies of the samples were calculated with eq 2. The results of the calculations are given in Table 3.

Standard Combustion Enthalpy of the Complex. The standard combustion enthalpy of the complex, $\Delta_c H_m^{\theta}$ (complex, s, 298.15K), refers to the combustion enthalpy change of the following ideal combustion reaction at 298.15 K and 100 kPa:

$$\mathrm{Er(C_5H_8NS_2)_3(C_{12}H_8N_2)(s)} + {}^{167}/_{4}\mathrm{O_2(g)} = {}^{1}/_{2}\mathrm{Er_2O_3(s)} + 27\mathrm{CO_2(g)} + 16\mathrm{H_2O(l)} + 6\mathrm{SO_2(g)} + {}^{5}/_{2}\mathrm{N_2(g)} \quad (10)$$

The standard combustion enthalpy of the complex was calculated with eqs 11 and 12

$$\Delta_c H_m^{\theta}(\text{complex, s, 298.15 K}) = \Delta_c U(\text{complex, s, 298.15 K}) + \Delta n RT \quad (11)$$

$$\Delta n = n_g(\text{products}) - n_g(\text{reactants}) \quad (12)$$

where n_g is the total number of moles of gas present as products or as reactants, R is 8.314 J K^{-1} mol^{-1}, and T is 298.15 K. The result of the calculation is −(15 450.0 ± 8.3) kJ mol^{-1}.

Standard Enthalpy of Formation of the Complex. The standard enthalpy of formation of the complex, $\Delta_f H_m^{\theta}$(complex, s, 298.15 K), is calculated with Hess' law according to the thermochemical equation given above.

$$\Delta_f H_m^{\theta}[\mathrm{Er(C_5H_8NS_2)_3(C_{12}H_8N_2)}, \mathrm{s}] = \left[\frac{1}{2}\Delta_f H_m^{\theta}(\mathrm{Er_2O_3, s}) + 27\Delta_f H_m^{\theta}(\mathrm{CO_2, g}) + 16\Delta_f H_m^{\theta}(\mathrm{H_2O, l}) + 6\Delta_f H_m^{\theta}(\mathrm{SO_2, g})\right] - \Delta_c H_m^{\theta}[\mathrm{Er(C_5H_8NS_2)_3(C_{12}H_8N_2)}, \mathrm{s}] \quad (13)$$

where $\Delta_f H_m^\theta(Er_2O_3, cr, 298.15\ K) = -(1900.1 \pm 6.5)$ kJ mol^{-1},[22] $\Delta_f H_m^\theta$ $(CO_2, g) = -(393.51 \pm 0.13)$ kJ mol^{-1}, $\Delta_f H_m^\theta$ $(H_2O, l) = -(285.830 \pm 0.042)$ kJ mol^{-1}, and $\Delta_f H_m^\theta(SO_2, g) = -(296.81 \pm 0.20)$ kJ mol^{-1}.[23,24] Its standard enthalpy of formation, $\Delta_f H_m^\theta$, is calculated to be $-(2478.9 \pm 9.7)$ kJ mol^{-1}.

4. Conclusions

The ternary complex formulated as $Er(C_5H_8NS_2)_3(C_{12}H_8N_2)$ has been synthesized in absolute ethanol by $ErCl_3 \cdot 3.46H_2O$ reacting with the mixed ligands of APDC and *o*-phen. The calorimetrical results at 298.15 K reflect the fact that the reaction in the liquid state occurs in a facile manner whereas the solid reaction does not.

The molar heat capacity of the complex, c_m, was determined to be (90.4 ± 1.5) J mol^{-1} K^{-1} at 298.15 K by using an RD-496 III heat conduction microcalorimeter. Through a designed thermochemical cycle, the standard molar enthalpy of reaction for the title solid-phase reaction was derived as being (16.1 ± 0.4) kJ mol^{-1}at 298.15 K.

On the basis of thermokinetic data of the liquid-phase reaction at different temperatures, the thermodynamic parameters and kinetic parameters of the reaction in the liquid state were obtained. The apparent activation energy of the reaction is higher than the activation energy of 63 kJ mol^{-1} at which the reaction occurs instantaneously at room temperature, showing that the title reaction proceeds feasibly in ethanol solution.

TG-DTG investigations indicate that the title complex is decomposed into Er_2S_3 and deposited carbon in one step, which provide a probe for the preparation of rare earth chalcogenide sulfide.

The standard enthalpy of formation of the title complex was determined to be $-(2478.9 \pm 9.7)$ kJ mol^{-1}, showing that the complex is quite thermally stable.

Literature Cited

(1) Mital, S. P.; Sharma, S. K.; Singh, R. V.; Tandon, J. P. Antifungal activity of some novel lanthanum thiosemicarbazone complexes. *Curr. Sci.* **1981**, *50*, 483−489.

(2) Tang, N.; Zhu, H. L.; Tan, M. Y. Studies on the complexes of rare earth with organic ligands containing sulphur atoms. *Acta Chim. Sin.* **1991**, *49*, 42−45.

(3) Jon, A.; Mccleverth; Gill, S.; Kowalski, R. S. Z.; Bailey, N. A.; Adams, H.; Lumbard, K. W.; Murphy, M. A. Aspects of the inorganic chemistry of rubber vulcanization. *J. Chem. Soc., Dalton Trans.* **1982**, 493−503.

(4) Jiang, T.; Zhang, W. G.; Shen, J. Y. Synthesis and vulcanizing properties of rare earth diethyldithiocarbaminate complexes. *J. Chin. Rare Earth Soc.* **2000**, *21*, 39−41.

(5) Ren, T. H.; Xia, J.; Zhong, J.; Zhang, W. G.; Li, K. B.; Zhang, Z. F. The tribological behaviors of a lanthanum complex with diethyldithiocarbamate ligand as additive in lithium grease. *Tribology* **1998**, *18*, 268−271.

(6) Gao, S. L.; Ji, M.; Chen, S. P.; Hu, R. Z.; Shi, Q. Z. J. The thermokinetics of the formation reaction of cobalt histidine complex. *Ther. Anal. Calorim.* **2001**, *66*, 423−429.

(7) Varand, V. L.; Glinskaya, L. A.; Klevtsova, R. F.; Larinov, S. V. Synthesis of mixed-ligand coordination compounds Sm(2,2′-Bipy)-$(S_2CN(C_2H_5)_2)_3$ and Smphen$(S_2CN(C_2H_5)_2)_3$, crystal structure of Sm(2,2′-Bipy) $(S_2CN(C_2H_5)_2)_3$. *Struct. Chem.* **2000**, *41*, 544−549.

(8) Su, C. Y.; Tan, M. Y.; Tang, N.; Gan, X. M.; Liu, W. S. Synthesis, structure and spectroscopic properties of complexes of rare earth dithiocarbamates with 2,2′-bipyridyl or 1, 10-phenanthroline. *J. Coord. Chem.* **1996**, *38*, 207−218.

(9) Varand, V. L.; Glinskaya, L. A.; Klevtsova, R. F. Synthesis and crystal and molecular structure of mixed-ligand compounds Eu-$(S_2CN(C_2H_5)_2)_3$(2, 2′-Bipy) and Eu$(S_2CN(C_2H_5)_2)_3$(1,10-phen). *Struct. Chem.* **1998**, *39*, 244−252.

(10) Su, C. Y.; Tang, N.; Tan, M. Y. Synthesis, properties and structure of lanthanide complexes with N,N-diethyldithiocarba-mate and 2,2′-bipyridyl. *Polyhedron* **1996**, *15*, 233−239.

(11) Coplen, T. B. Atomic weights of the elements. *J. Phys. Chem. Ref. Data* **2001**, *30*, 701−712.

(12) Ji, M.; Liu, M. Y.; Gao, S. L.; Shi, Q. Z. The enthalpy of solution in water of complexes of zinc with methionine. *Instrum. Sci. Technol*. **2001**, *29*, 53−57.

(13) Kilday, M. V. The enthalpy of solution of SRM 1655 (KCl). *J. Res. Natl. Bur. Stand*. (*U.S.)* **1980**, *85*, 467−481.

(14) Yang, X. W.; Chen, S. P.; Gao, S. L.; Li, H. Y.; Shi, Q. Z. Combustion of rotating − bomb combustion calorimeter and measurement of thermal effects. *Instrum. Sci. Technol*. **2002**, *30*, 311−315.

(15) Popov, M. M. *Thermometry and Calorimetry*; Moscow University Publishing House: Moscow, 1954; p 382.

(16) Dong, Q. N. *IR Spectroscopy*; Chemical and Industrial Press: Beijing, 1979; p 99.

(17) Nakamoto, K. *Infrared and Raman Spectra of Inorganic and Coordination Compounds*, 4th ed.; Chemical and Industrial Press: Beijing, 1991; p 253; translated by D. J. Huang, R. Q. Wang.

(18) Nakamoto, K.; Fujito, J.; Condrate, R. A. Infrared spectra of metal chelate compounds. IX. A normal coordinate analysis of dithiocarbamate complexes. *Chem. Phys.* **1963**, *39*, 423−426.

(19) Trindade, T.; O'Brien, P.; Pickett, N. L. Nanocrystalline semiconductors: synthesis, properties and perspectives. *Chem. Mater.* **2001**, *13*, 3843−3858.

(20) Ditmars, D. A.; Ishihara, S.; Chang, S. S.; Bernstein, G. Enthalpy and heat-capacity standard reference material: synthetic sapphire (α-Al_2O_3) from 10 to 2250 K. *J. Res. Natl. Bur. Stand. (U.S.)* **1982**, *87*, 159−163.

(21) Rojas Aguilar, A.; Orozco Guareno, E. Thermochemistry of methyl-D-glucopyranosides and methyl-D-galactopyranosides. *J. Chem. Thermodyn.* **2000**, *32*, 767−775.

(22) Cordfunke, E. H. P.; Kongings, R. J. M. The enthalpies of formation of lanthanide compounds. III. Ln_2O_3 (cr). *Thermochim. Acta* **2001**, *375*, 65−79.

(23) Cox, J. D.; Angman, D. D.; Medvedev, W. V. A. *CODATA Key Values for Thermodynamics*; Hemisphere: New York, 1989.

(24) Cox, J. D. CODATA recommended key values for thermodynamics, 1977 Report of the CODATA task group on key values for thermodynamics, 1977. *J. Chem. Thermodyn.* **1978**, *10*, 903−906.

Received for review December 5, 2004. Accepted May 12, 2005. We gratefully acknowledge the financial support of the National Natural Science Foundation of China (Grant 20171036), Education Committee of Shaanxi Province (Grants 01JK229 and FF02328).

JE0495738